HZB Helmholtz Zentrum Berlin

Victor Ukleev
BESSY II, Helmholtz-Zentrum Berlin für Materialien und Energie
Department of Spin and Topology in Quantum Materials

Long-periodic spin textures in vector magnetic fields as seen by resonant elastic x-ray scattering

YRLG Workshop
Ingelheim
26-07-2023

Topological spin orders in magnetic materials

Particle-like spin objects hosting "topological charge": a zoo of the topological spin textures

Theoretically proposed topological spin orders: $n = \frac{1}{4\pi}\int \mathbf{M}\cdot\left(\frac{\partial \mathbf{M}}{\partial x}\times\frac{\partial \mathbf{M}}{\partial y}\right)\mathrm{d}x\mathrm{d}y$

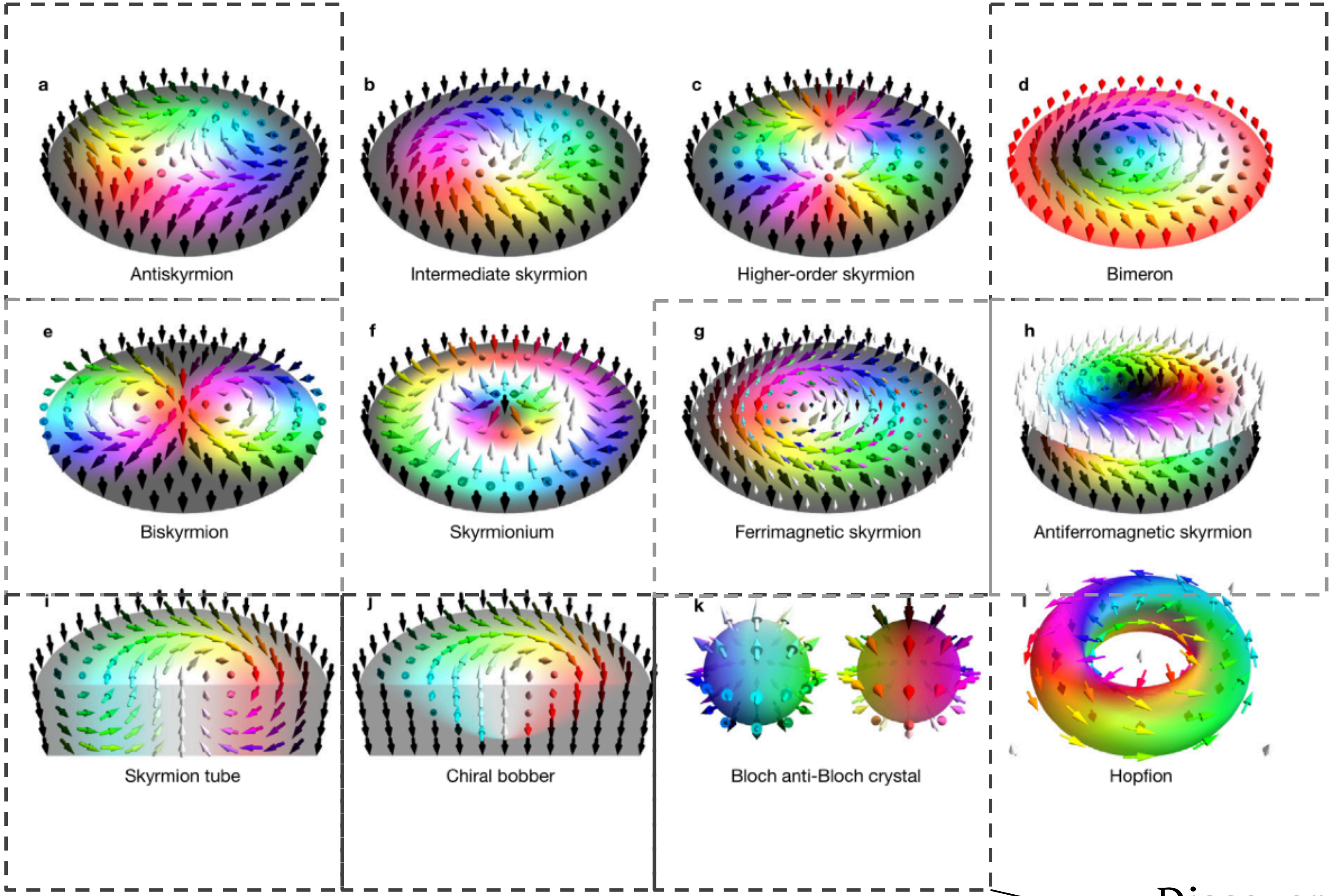

Discovered in bulk materials

G. Börge, I. Mertig, and O. A. Tretiakov. Physics Reports 895, 1-28 (2021)

Topological spin orders in magnetic materials

- Topological spin textures and emergent fields

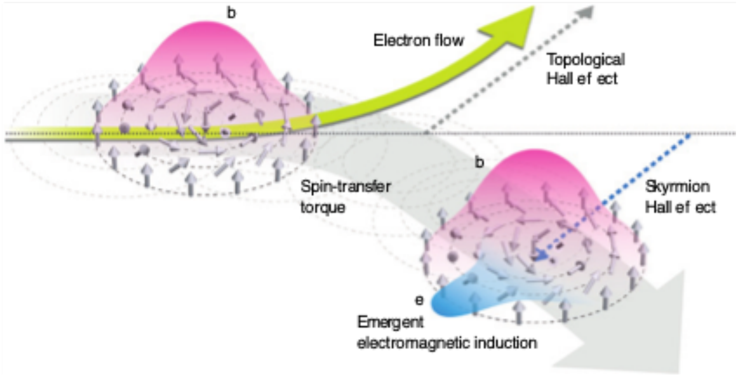

Electrons adiabatically traversing the topological spin texture adapt to the local **M** and acquire a quantum-mechanical Berry phase

Emergent magnetic field $\mathbf{B}_i^e = \frac{\hbar}{2}\epsilon_{ijk}\hat{n}\cdot(\partial_j\hat{n}\times\partial_k\hat{n})$

Emergent electric field $\mathbf{E}_i^e = \hbar\hat{n}\cdot(\partial_i\hat{n}\times\partial_t\hat{n})$

Topological contribution to the Hall resistivity:

$$\rho_{yx} = R_0 B + R_S M + \rho_{yx}^T$$

normal — anomalous — topological

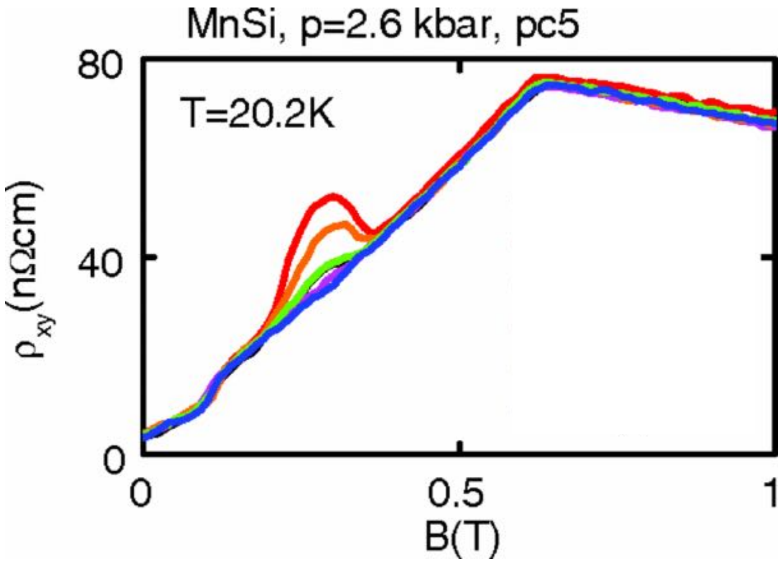

The effective field in MnSi (skyrmion size of 15 nm)

$$B^{\text{eff}} = -\frac{h}{e}\left(\frac{\sqrt{3}}{2\lambda_S^2}\right) \approx -13.15\ \text{T}.$$

generated by the applied field of 0.3 T!

Ritz, R., et al. Physical Review B 87.13 134424 (2013)

Topological spin orders in magnetic materials

- Potential applications

Racetrack memories

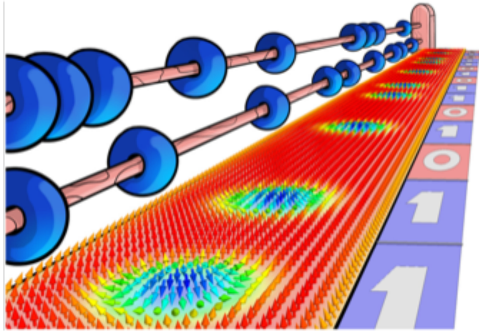

K. Everschor-Sitte, et al. J. Appl. Phys. 124, 240901 (2018)

GHz and THz nano-oscillators

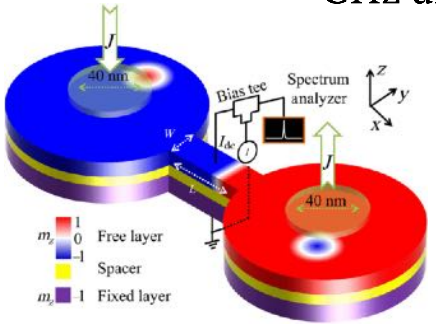

C. Jin, et al. Phys. Rev. App. 9, 044007 (2018)

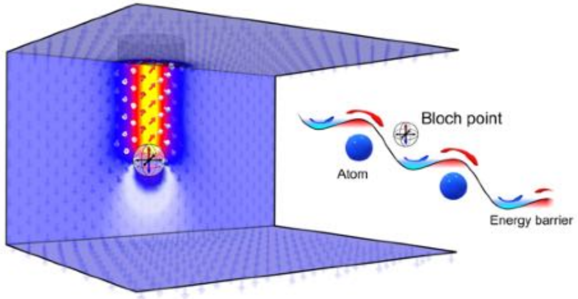

Y. Li, et al. Phys. Rev. Res., 2, 033006 (2020)

Unconventional computing

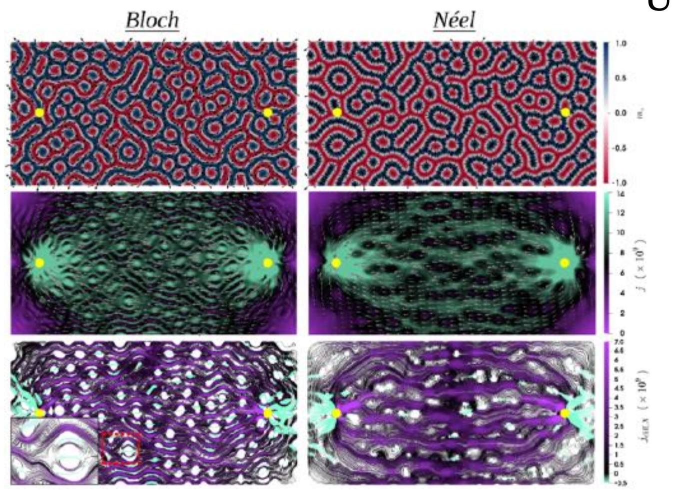

K. Everschor-Sitte, et al. AIP Advances 8, 055602 (2018)

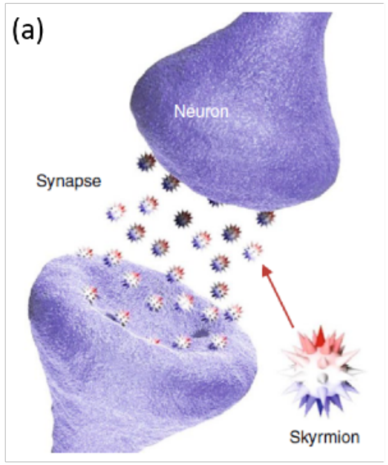

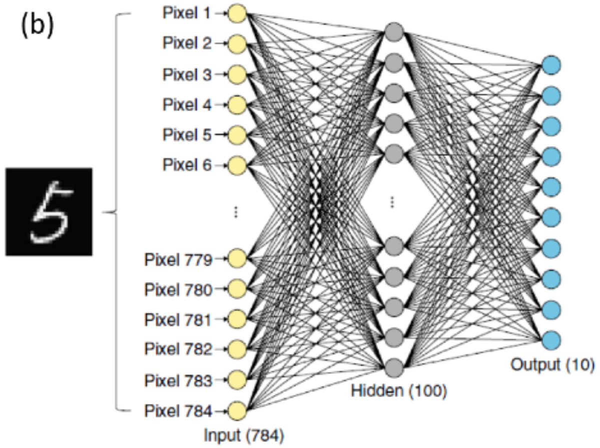

K.M. Song, et al. Nature Electronics 3, 3 148-155 (2020)

Resonant x-rays for magnetism

Polarised x-rays - a tool to study static and dynamics magnetic orders

contrast mechanism for ‘soft’ x-rays (~100-2000 eV) - XMCD

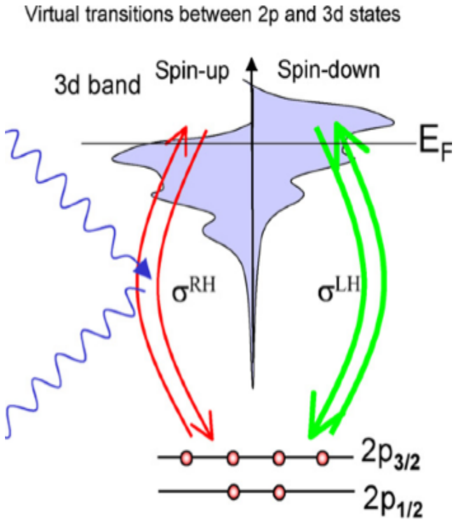

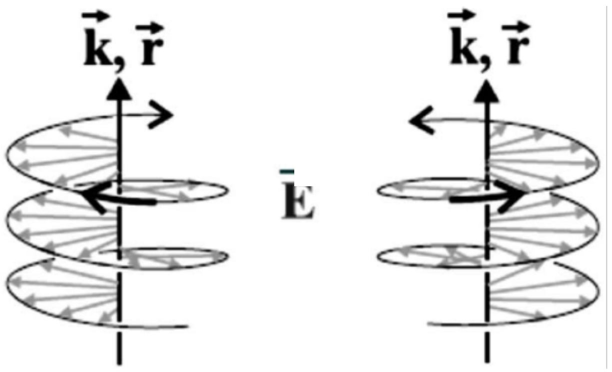

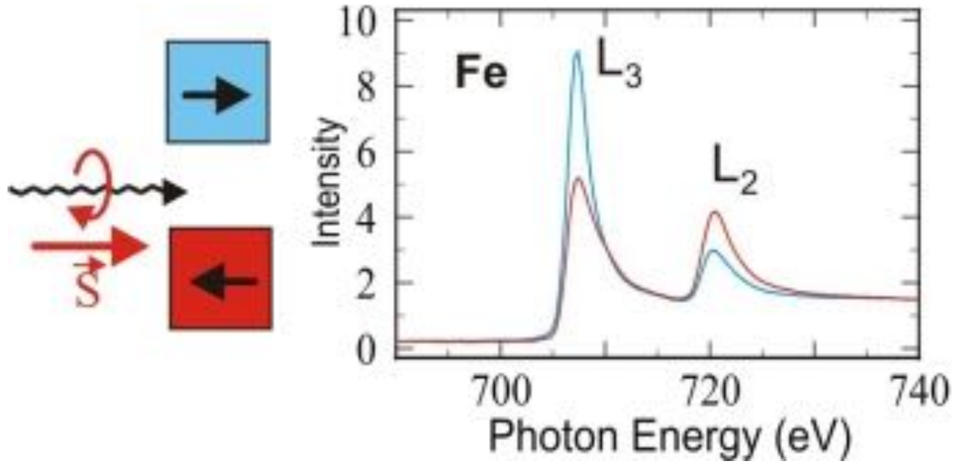

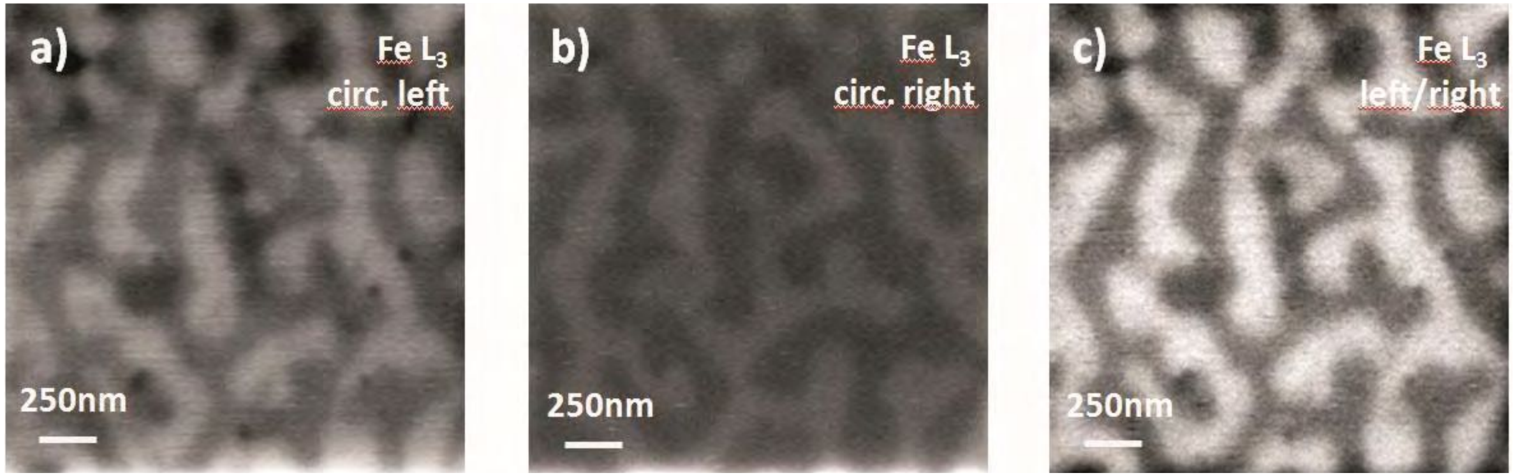

$$I(z) = I_0\, e^{-\mu_x\, z}$$

where μ is material-specific coefficient dependent on photon energy

XMCD microscopy, diffraction, scattering, etc.

IEEE Trans. on Magn. 2015, 51, 2 https://www-ssrl.slac.stanford.edu/stohr/

Resonant x-rays for magnetism (scattering)

- 3*d*-2*p* transition is used for resonant scattering and diffraction: $L_{2,3}$ edges of TM correspond to soft x-rays in the energy range of 460 (Ti L_3) – 950 eV (Cu L_2) and wavelength range λ ~ 13-27 Å
- Resonant x-rays allow both reciprocal (scattering) and real-space (imaging)

Thickness: transmission vs magnetic scattering intensity

$$I_{mag} \sim M^2 = (\mu A z)^2$$

$$I_{trans} = I_0 exp(-l_{att} z)$$

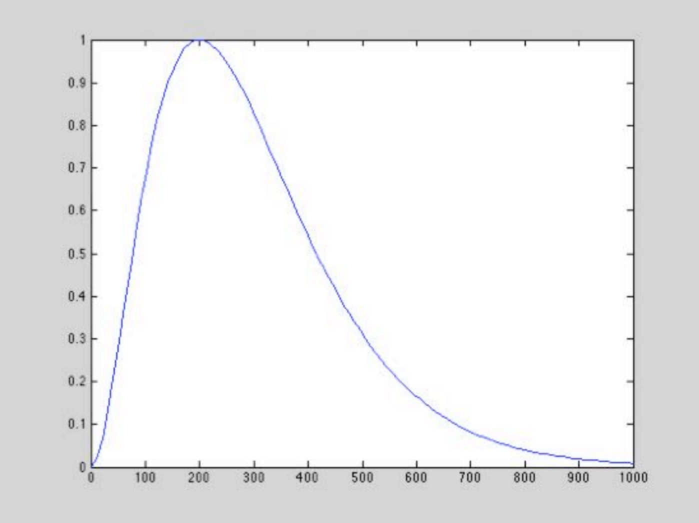

Limited by a few 100s of nm

charge *magnetic*

$$f^n = (\boldsymbol{e}_n \cdot \boldsymbol{e}'_n) f^n_c + i(\boldsymbol{e}_n \times \boldsymbol{e}'_n) \cdot \boldsymbol{M}^n f^n_{m1} + (\boldsymbol{e}_n \cdot \boldsymbol{M}^n)(\boldsymbol{e}'_n \cdot \boldsymbol{M}^n) f^n_{m2}.$$

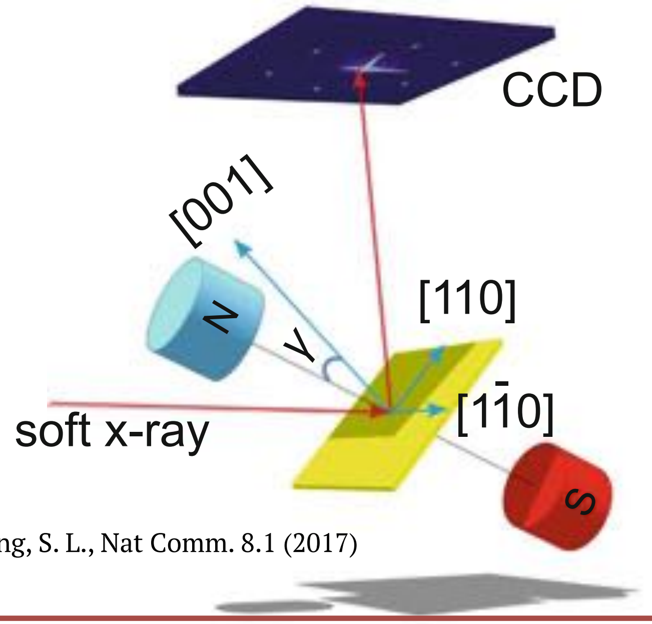

Zhang, S. L., Nat Comm. 8.1 (2017)

Rather weak effect (need a bright x-ray source)

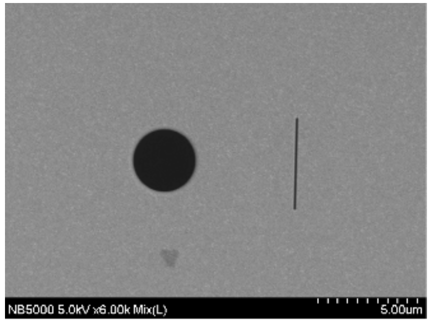

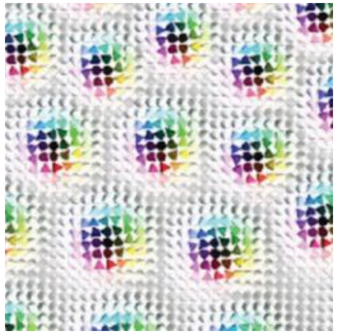

$$\frac{\sigma_m}{\sigma_c} \sim 10^{-2}$$

charge *magnetic*

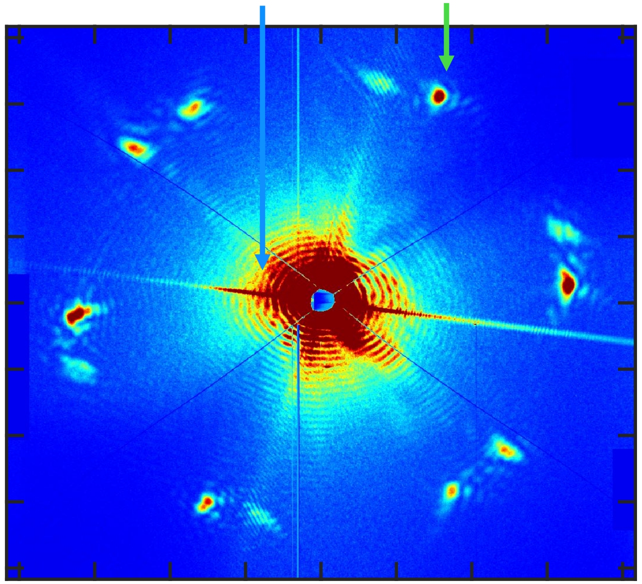

1 μm-thick Cu_2OSeO_3

V.U., unpublished

Small-angle scattering: a tool to study nanometric orders

SANS (neutrons)

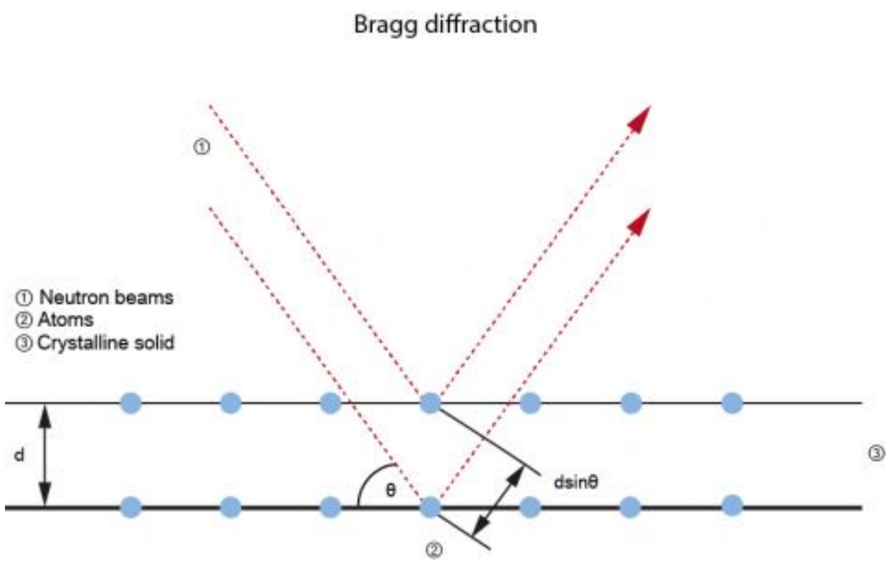

typical SANS setting

λ~5 Å
d~800 Å
θ~0.2º - small!

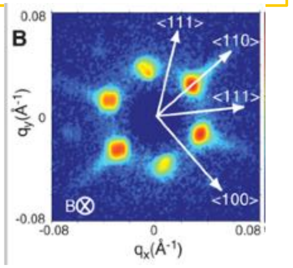

pixel size ~ 1x1 cm²

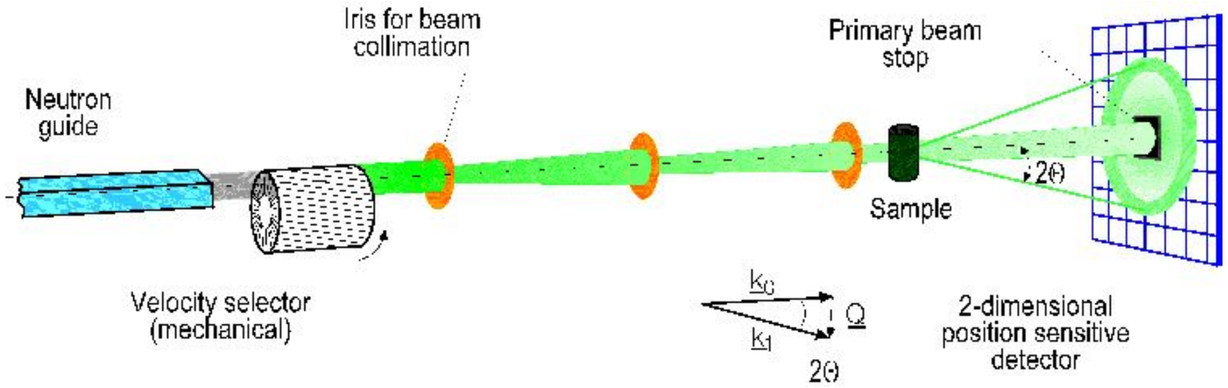

Large instrument!

SAXS (resonant x-rays)

Also known as:

Resonant Elastic X-ray Scattering (REXS)
X-ray Magnetic Resonant Scattering (XRMS)
Resonant X-ray Magnetic Scattering (RXMS)
Soft X-ray Magnetic Resonant Scattering (SXRMS)
Resonant Magnetic Small-angle X-ray Scattering (RMSAXS)
Small-angle Resonant Elastic X-ray Scattering (SAREXS)
Transmission REXS (T-REXS)
Anomalous Small-angle X-ray Scattering (ASAXS)
Resonant Soft X-ray Scattering (RSoXS), etc.

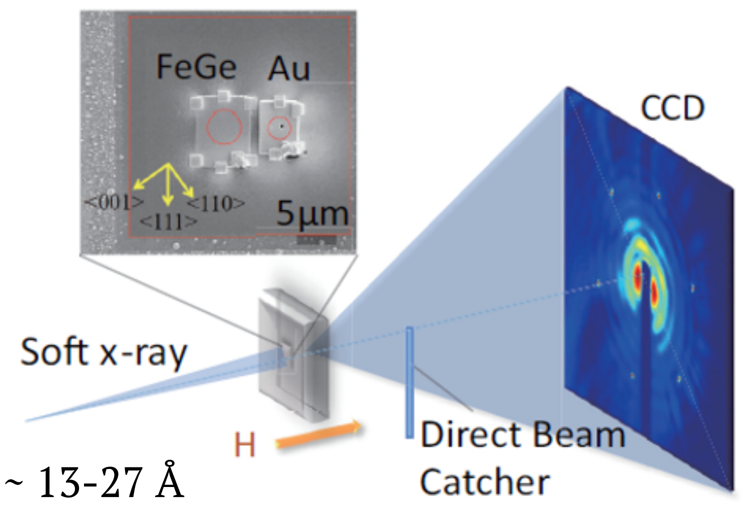

λ ~ 13-27 Å

pixel size ~ 15x15 μm²

https://www.psi.ch/sinq/sansi/components
Yamasaki, Y., et al., PRB 92.22 (2015): 220421

Sample preparation for soft x-ray experiment

- Sample size and shape are adjusted according to the attenuation length of soft x-ray beam (~50 - 1000 nm thick for TM) and desire to use the coherence (aperture size of 1-20 µm)
- Method: thin plates prepared by Focused Ion Beam (FIB) milling

Commercial membranes (Silson Ltd., UK)
50 - 500 nm

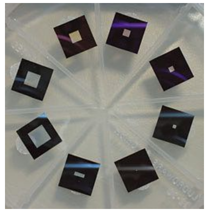

Silicon nitride is almost transparent for soft x-rays

1 µm Au-coated Si_3N_4 membranes

Zeiss NVision at EMF PSI

Sample preparation for soft x-ray experiment

- Sample size and shape are adjusted according to the attenuation length of soft x-ray beam (~50 - 1000 nm thick for TM) and desire to use the coherence (aperture size of 1-20 μm)
- Method: thin plates prepared by Focused Ion Beam (FIB) milling

Membrane preparation

Si_3N_4 membrane: thickness of 200 nm (transparent for soft X-rays)

Coating membrane with a few micron of Au to block the beam

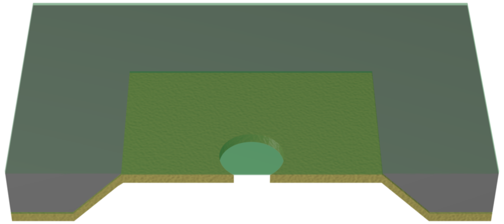

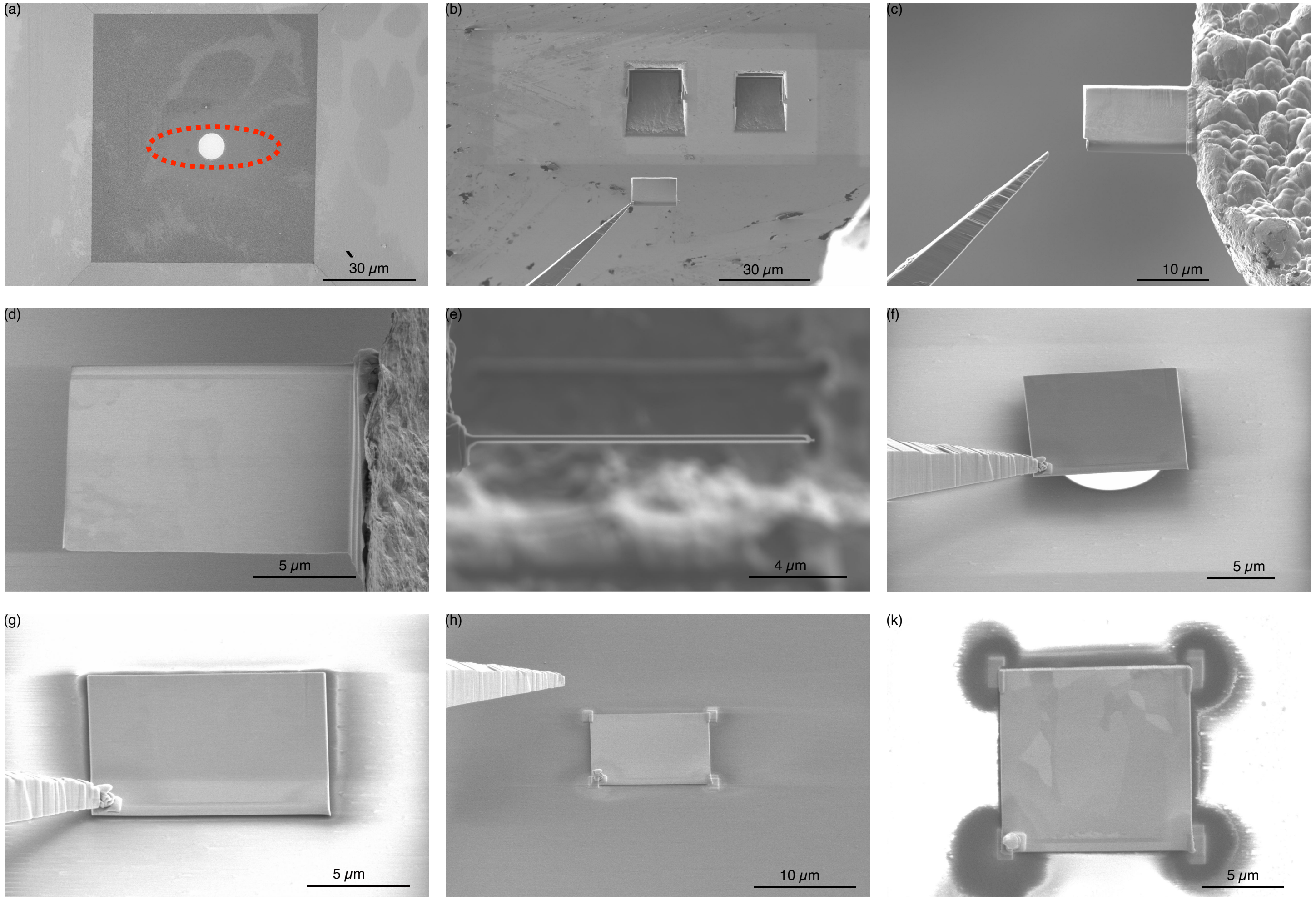

Büttner, F., et al., Optics express, 21(25), pp.30563-30572.

BESSY-II, Helmholtz-Zentrum Berlin for Materials and Energy

- **Location:** Adlershof, Berlin, Germany
- **Operator:** Helmholtz-Zentrum Berlin für Materialien und Energie (Financing: 90% federal government, 10% State of Berlin)
- **Commissioned:** September 1998

- **Upgrades:** October 2012: Top-up mode and fast-orbit feedback
- **Circumference:** 240 metres
- **Bending magnets**: 32
- **Beam tubes:** approx. 45
- **Electron energy:** 1.7 gigaelectronvolts (GeV)
- **Nominal beam current:** 300 milliamperes (mA)
- **Energy of the synchrotron radiation**: 1 to 150 kiloelectronvolts (keV)
- **Duration of the light pulse:** 20 picoseconds (after the upgrade to BESSY VSR: 1.5 and 15 ps)

- **Measurement time per year:** 40 weeks p.a., approx. 6,600 hours or 800 shifts p.a. (2017)
- **User visits from guest researchers**: 3,000 p.a.
- **Strategic partners:** Max Planck Society, PTB, BAM, Berliner universities

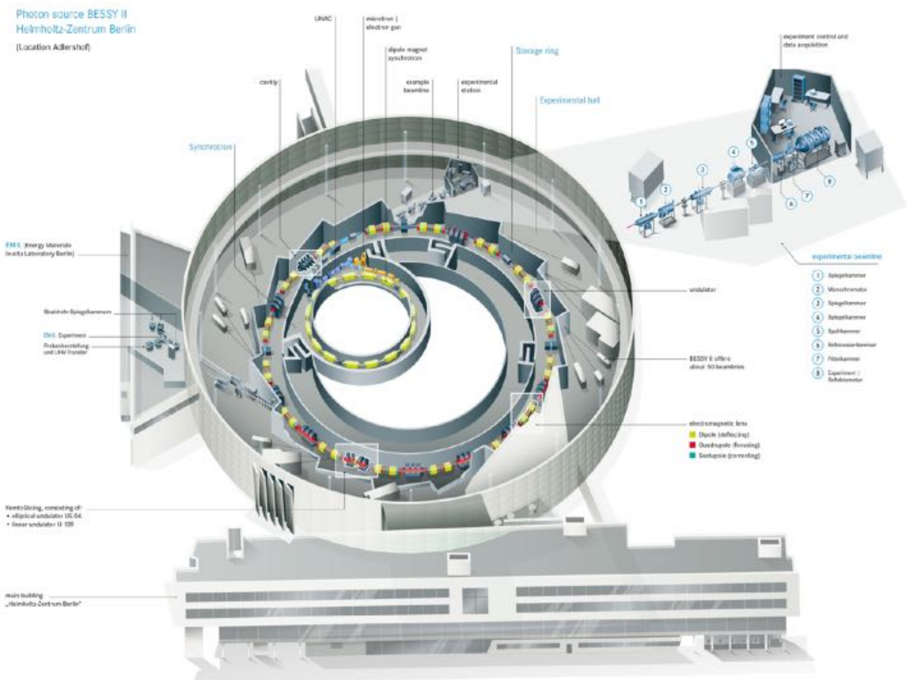

https://www.helmholtz-berlin.de/forschung/quellen/bessy/bessy-in-zahlen_en.html

PM-2 VEKMAG, Dep. Spin and Topology in Quantum Materials

Instrument scientist: Dr. Florin Radu

Dr. Victor Ukleev

Dr. Chen Luo

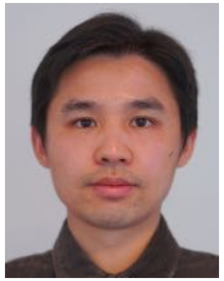

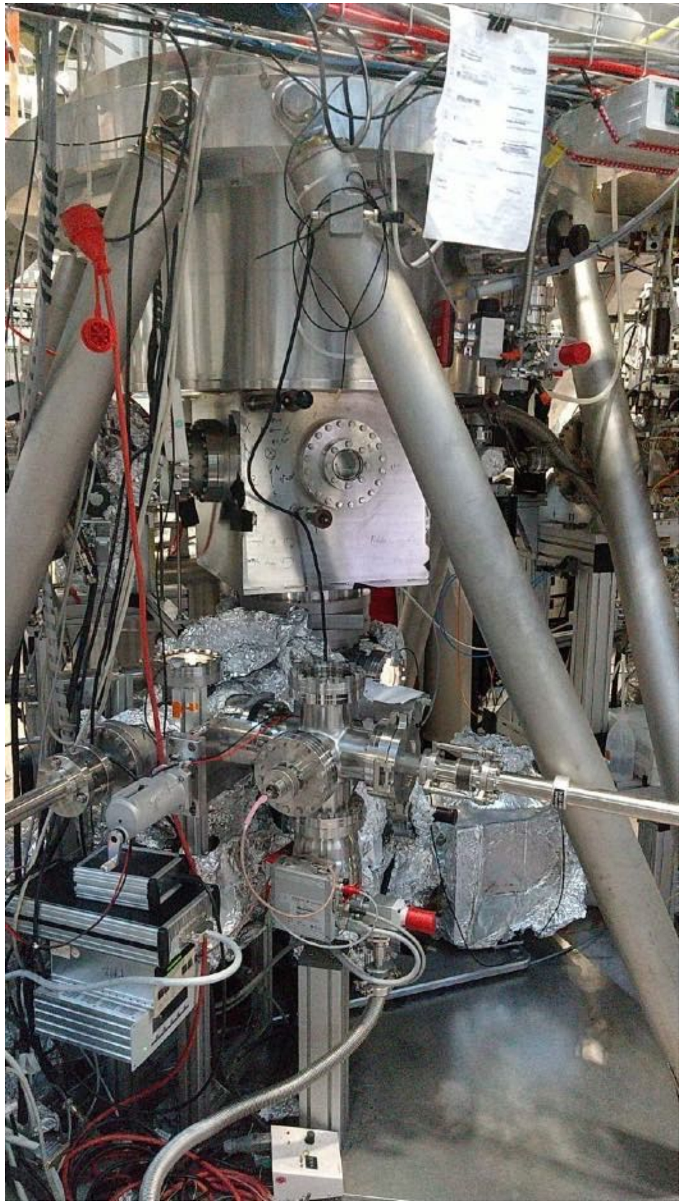

PM-2 beamline:

- **Source:** Dipole
- **Energy range:** 20-1600 eV
- **Flux:** $\sim 5 \cdot 10^9$ photons/sec
- **Polarization:** 77% circular, linear horizontal
- **Focus:** from 60x50 μm to 800x800 μm
- **Beam availability**: 24 h/d, 6 d/w, 40 w/y
- **User beam:** ~70%

VEKMAG instrument:

- **Pressure:** $\sim 10^{-9}$ mbar
- **Temperature:** 350 mK - 500 K
- **Magnetic field**: 9 T (X), 2 T (Y), 1 T (Z), up to 1 T in any 3D direction
- **Sample manipulator**: *x*, *y*, *z*, θ, azimuthal (ext. holder)
- **Detectors:** drain current: TEY, photodiodes: FY, transmission, reflection (*z*, 2θ), 2k-CCD, 4k-CCD (scattering in transmission).
- **Techniques:** XAS, XMCD, XLMD, XFMR, XRMS, SAXS
- **Unique capabilities:** downstream deposition chamber for in-situ experiments and vacuum transfer; in-situ cleaving; electric transport capability; XFMR; SAXS; laser (to be commissioned in 2023-2024)

https://www.helmholtz-berlin.de/pubbin/igama_output?modus=einzel&sprache=en&gid=1969&typoid=75136

https://www.helmholtz-berlin.de/pubbin/igama_output?modus=einzel&sprache=en&gid=1937&typoid=75136

High-resolution SAXS for capturing weak effects in cubic helimagnets

Bak-Jensen model of B20s:

$$H_{\rm EX} = -\frac{1}{2}\sum J_{\mathbf{R}-\mathbf{R}'}\mathbf{S}_{\mathbf{R}}\cdot\mathbf{S}_{\mathbf{R}'};$$

$$H_{\rm DM} = \frac{1}{2}\sum D_{\mathbf{R}-\mathbf{R}'}(\nabla-\nabla')[\mathbf{S}_{\mathbf{R}}\times\mathbf{S}_{\mathbf{R}'}];$$

$$H_{\rm AE} = \frac{1}{2}\sum F_{\mathbf{R}-\mathbf{R}'}\{(\nabla_x S^x_{\mathbf{R}})(\nabla'_x S^x_{\mathbf{R}'}) + (\nabla_y S^y_{\mathbf{R}})(\nabla'_y S^y_{\mathbf{R}'}) + (\nabla_z S^z_{\mathbf{R}})(\nabla'_z S^z_{\mathbf{R}'})\};$$

$$H_Z = -\mathbf{H}\sum \mathbf{S}_{\mathbf{R}},$$

$$H_{\rm CA} = K\sum\{(S^x_{\mathbf{R}})^4 + (S^y_{\mathbf{R}})^4 + (S^z_{\mathbf{R}})^4\}.$$

Helical state

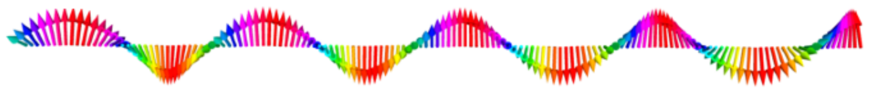

Conical state $\vec{B}$

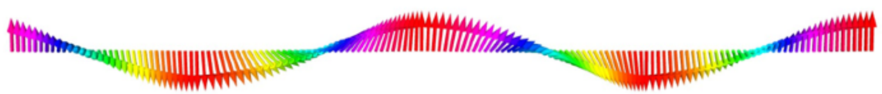

spiral wavector $k = 2\pi/l$

$$k = S\frac{D}{A}\left(1 - \frac{SF}{2A}L(\hat{k})\right) \approx S\frac{D}{A},$$

standard "D/J"

"weak" AEI contribution (a few % to D/J)

L - Cubic invariant:

$$\sin^2\vartheta(\sin^2\varphi\cos^2\varphi + \cos^2\vartheta),$$

2/3 for [111], 0 for [100]

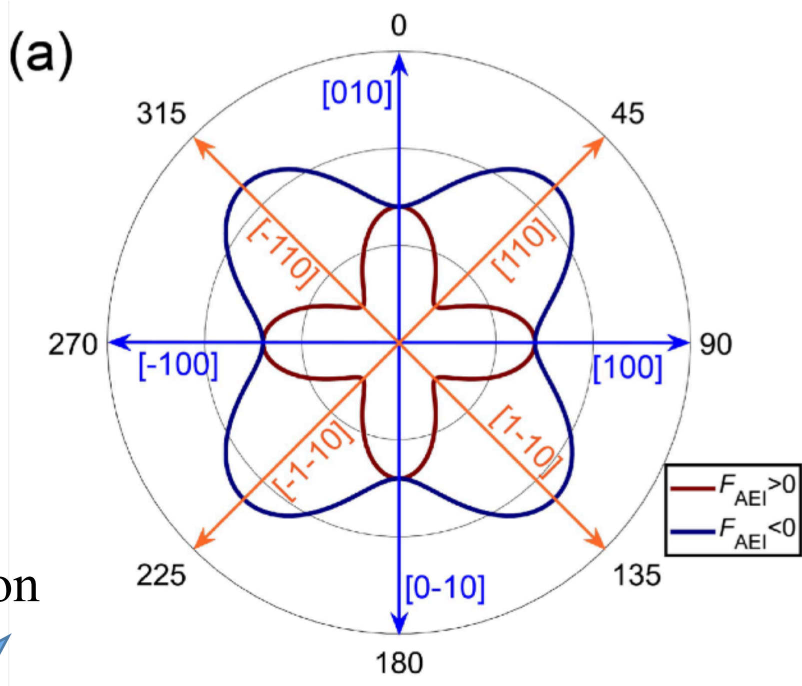

Anisotropic k-vector in the (001) plane

The k-vector anisotropy is the only way to isolate the AEI

P. Bak and M. H. Jensen, J. Phys. C 13, L881 (1980)
S.V. Grigoriev, et al. PRB 91.22, 224429 (2015)

EXAMPLE I

High-resolution SAXS for capturing weak effects in cubic helimagnets

- Recently, we proposed a SAXS-based method to unambiguously quantify the AEI constant via tuning the spiral orientation by the vector field
- Anisotropic exchange interaction is called to explain the new tilted conical and low-T skyrmion phases in cubic chiral insulator Cu_2OSeO_3

Recent data on FeGe

$$\mathbf{Q} = \frac{SD\hat{c}}{A_{ex}}\left(1 - \frac{SFI(\hat{c})}{2A_{ex}}\right),$$

$$I(\hat{c}) = I(\theta) = \frac{\sin^2\theta(1 + 3\cos^2\theta)}{2}.$$

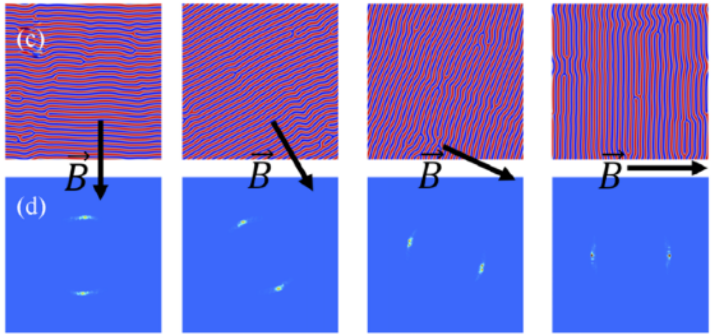

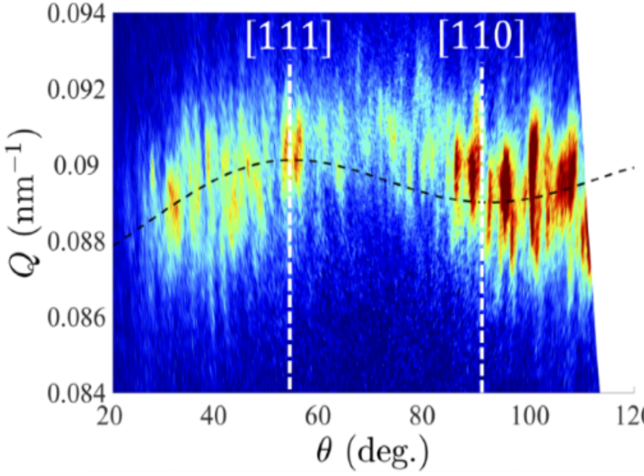

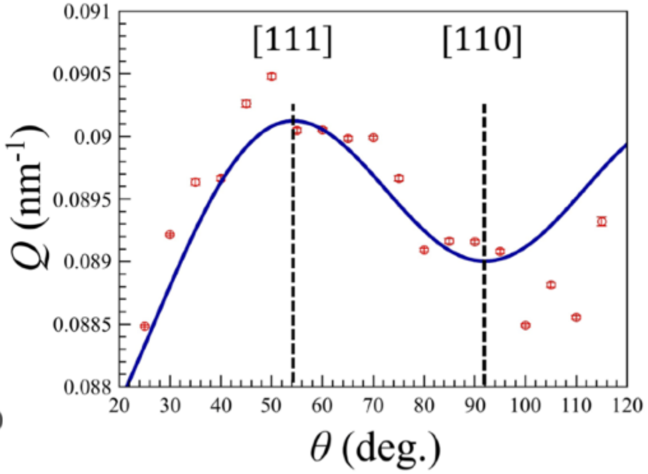

PHYSICAL REVIEW RESEARCH 3, 013094 (2021)

Signature of anisotropic exchange interaction revealed by vector-field control of the helical order in a FeGe thin plate

Victor Ukleev,[1,*] Oleg Utesov,[2,3,4] Le Yu,[1,5,6] Chen Luo,[7] Kai Chen,[7] Florin Radu,[7] Yuichi Yamasaki,[8,9] Naoya Kanazawa,[10] Yoshinori Tokura,[10,11,12] Taka-hisa Arima,[11,13] and Jonathan S. White[1]

What about Cu_2OSeO_3?

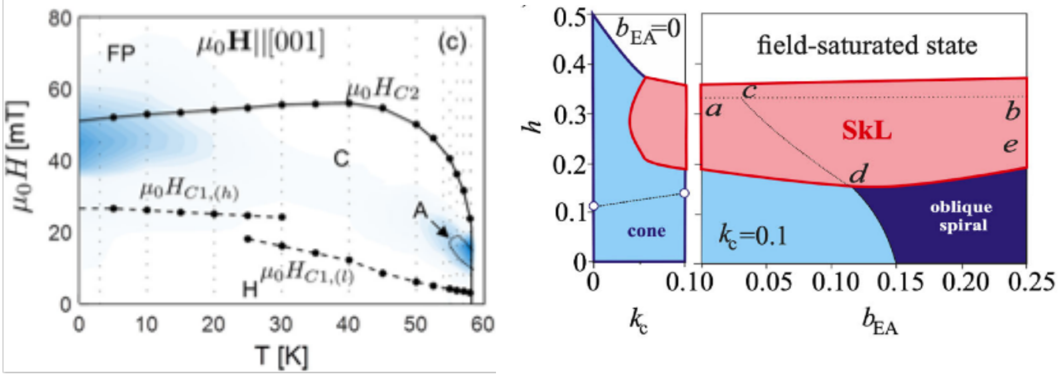

F. Qian, et al., Science Advances 4.9 (2018): eaat7323.

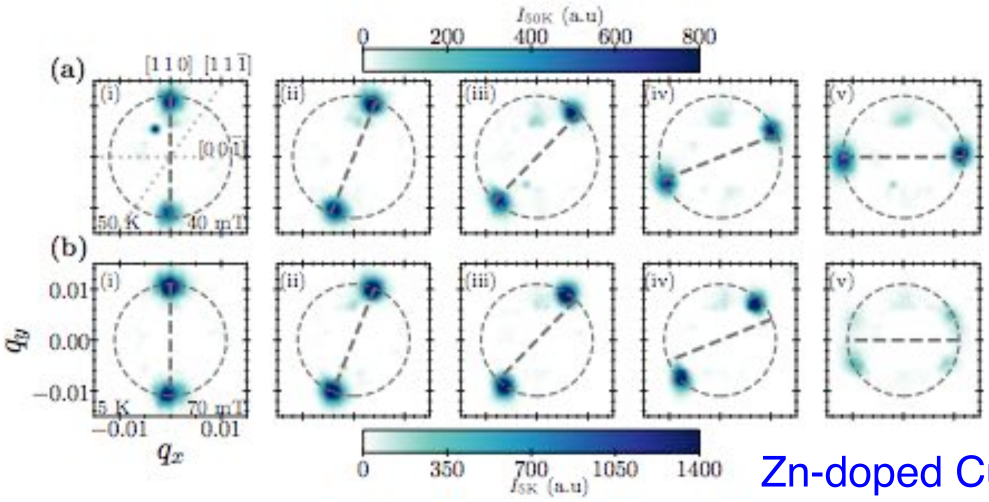

Zn-doped Cu_2OSeO_3

S. H. Moody, et al., Phys. Rev. Research 3, 043149 (2021)

High-resolution SAXS for capturing weak effects in cubic helimagnets

Cu_2OSeO_3 is a $P2_13$ cubic chiral magnet with the spiral period of 60 nm

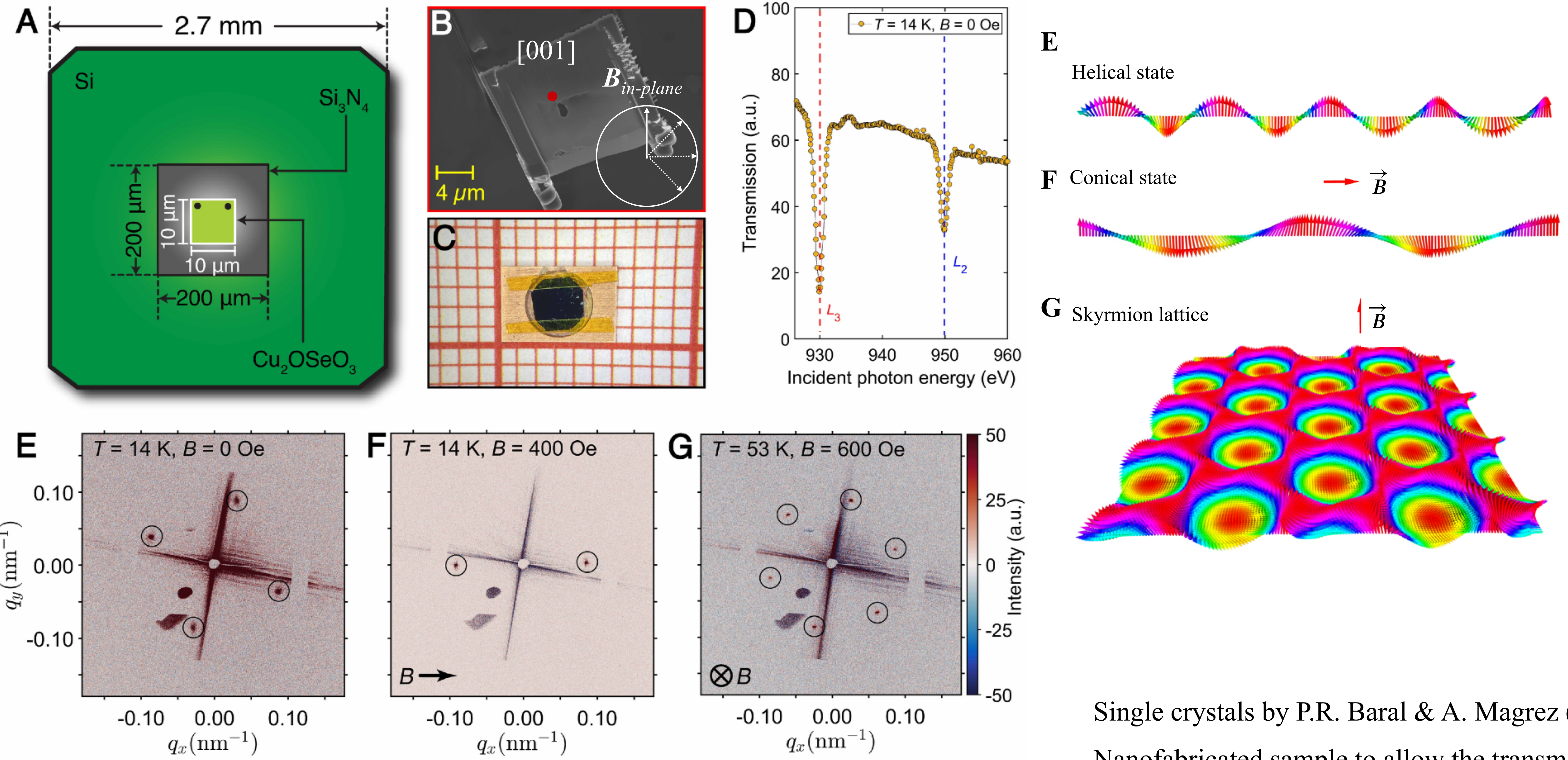

Single crystals by P.R. Baral & A. Magrez (EPFL)

Nanofabricated sample to allow the transmission

High-resolution SAXS for capturing weak effects in cubic helimagnets

Individual images of the conical states with 3 deg. step

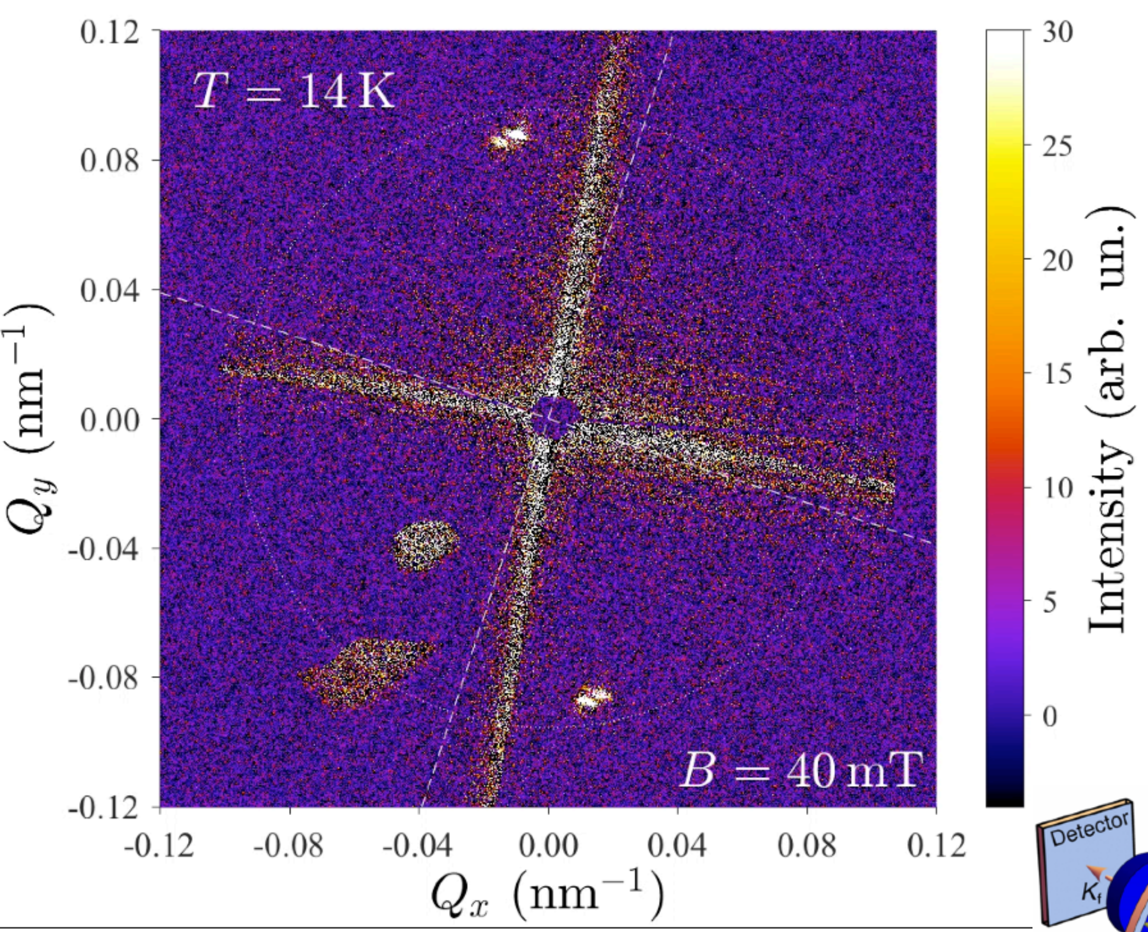

Summed image at 14 K

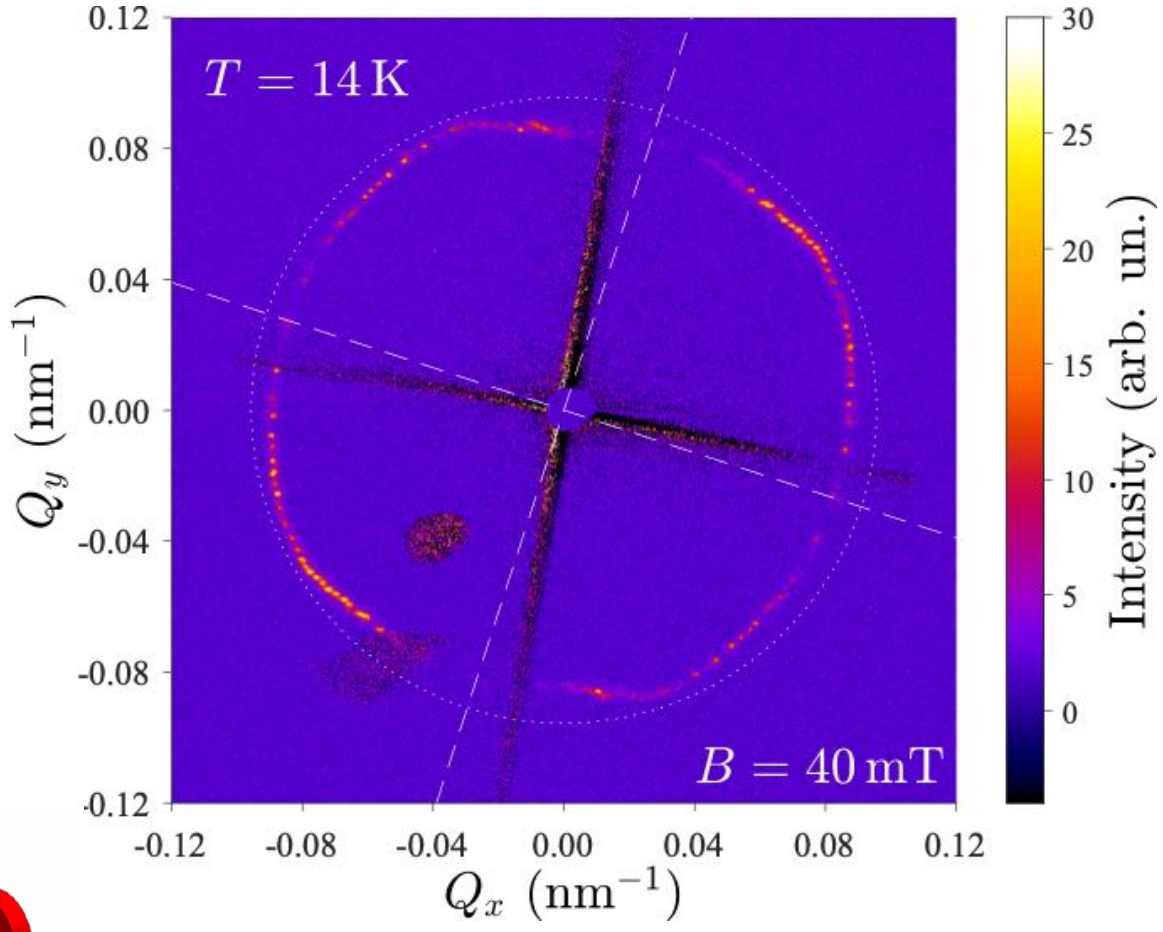

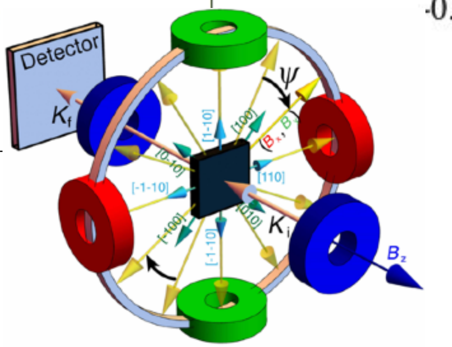

Peaks are not lying at the same |Q|!

High-resolution SAXS for capturing weak effects in cubic helimagnets

Summed pattern for all vector field angles

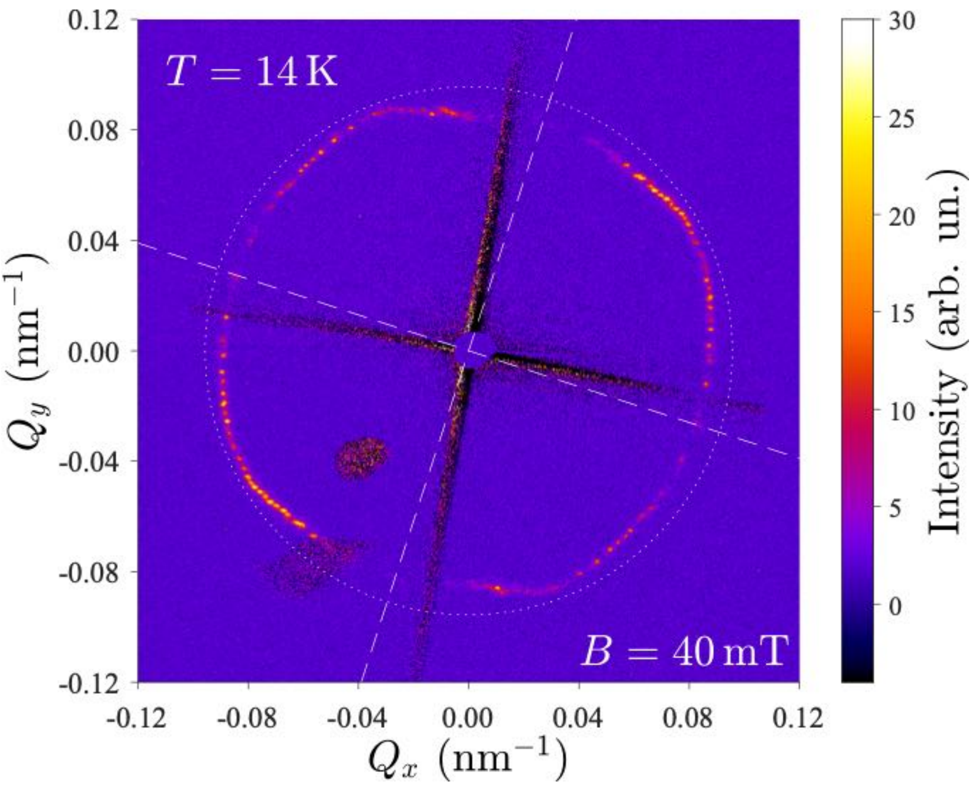

Fitted peak position

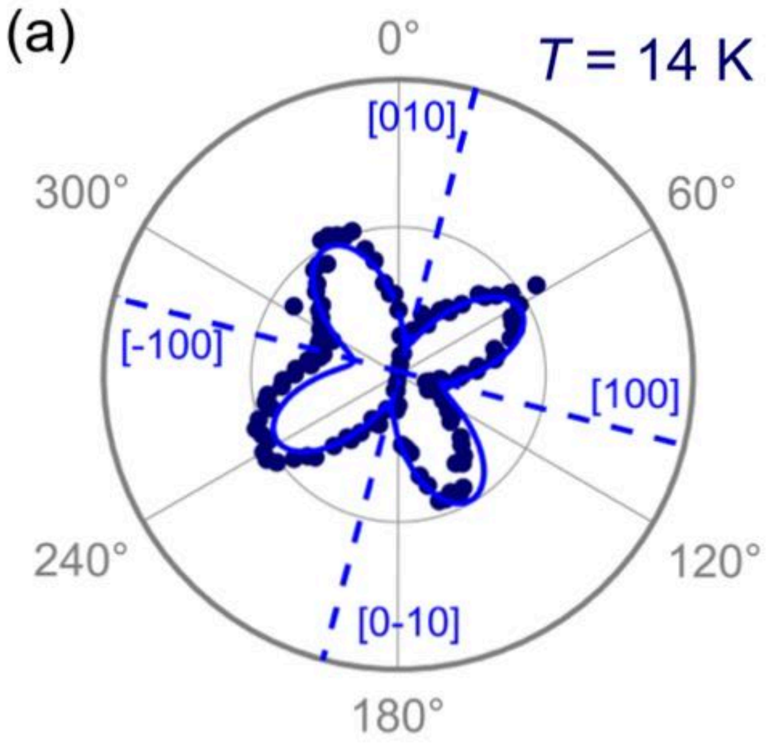

50 K vs. 14 K

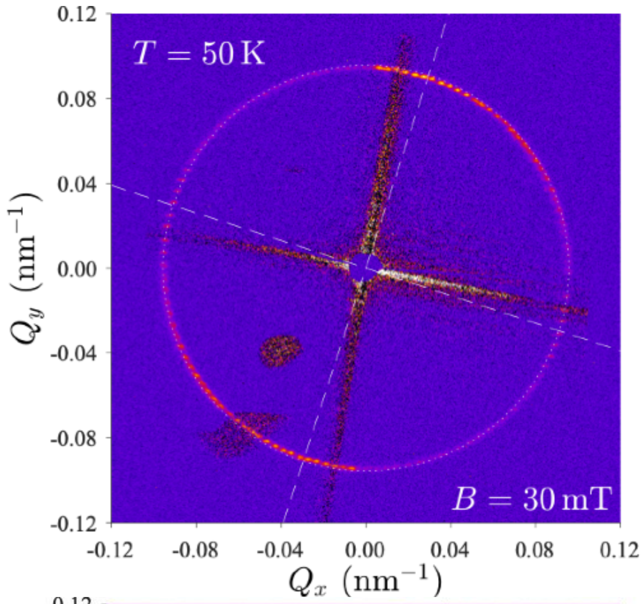

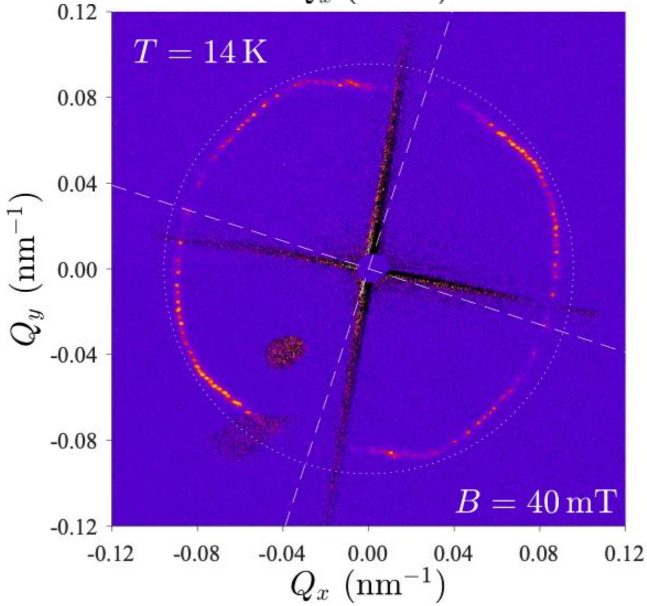

Strongly anisotropic periodicity of the conical texture!

Q is minimum for <100> and maximum for <110> -> F>0

$$Q = Q_0\left\{1 - \frac{F_{\mathrm{AEI}}\sin^2 2\psi}{4J}\right\} - \frac{JZ^2\cot^2\alpha}{2D^3}\sin^2 2(\psi-\phi)$$

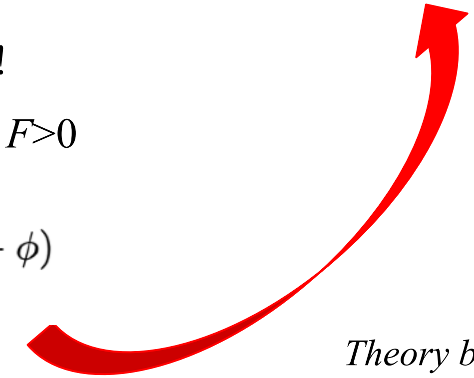

Theory by O. Utesov (IBS, Korea Rep.)

High-resolution SAXS for capturing weak effects in cubic helimagnets

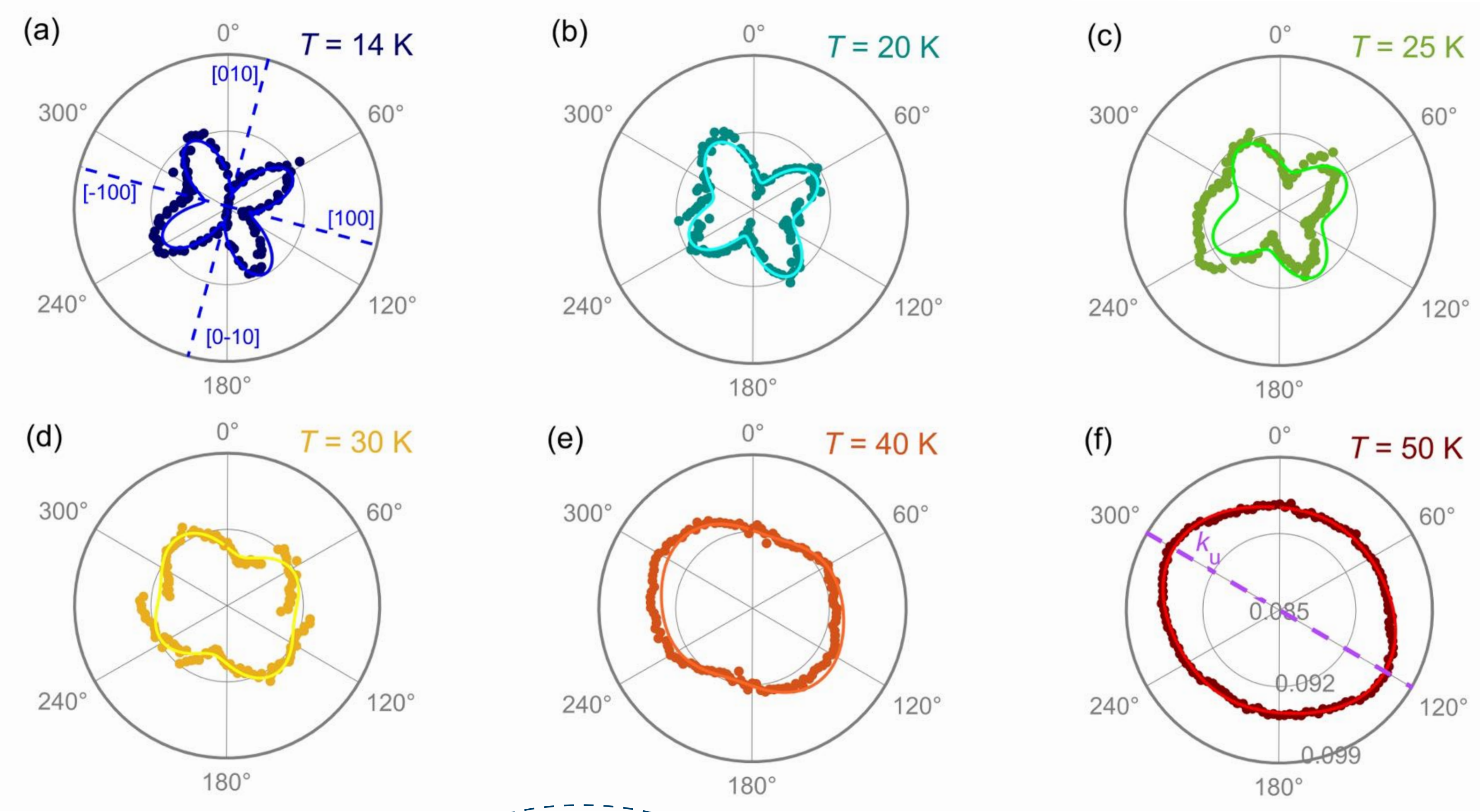

$$Q = Q_0\left\{1 - \frac{F_{\mathrm{AEI}} \sin^2 2\psi}{4J}\right\} - \frac{JZ^2 \cot^2 \alpha}{2D^3} \sin^2 2(\psi - \phi)$$

Anisotropy gradually vanishes on warming to 50 K (T_c = 55 K), but a weak uniaxial distortion is present due to the tensile strain

F* vs *T

Dramatic increase compared to the Zn-doped COSO

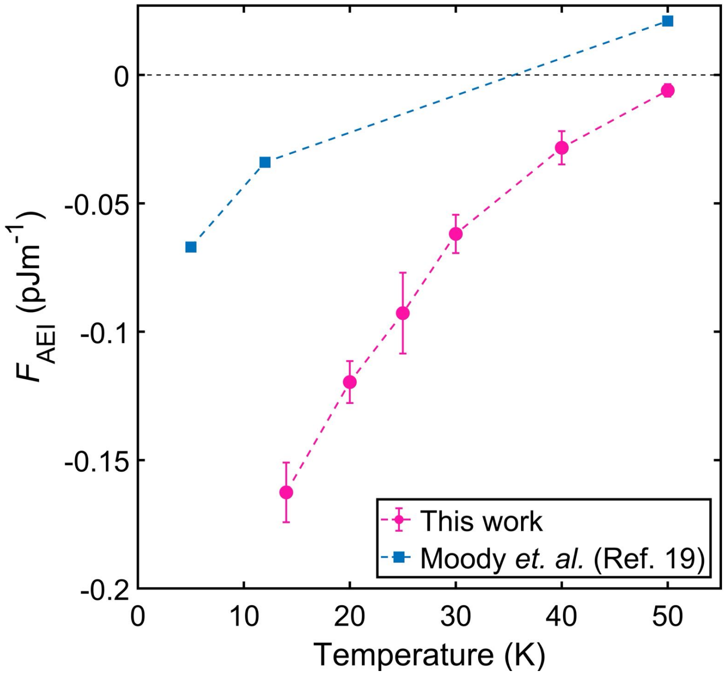

Reciprocal space resolution and acquisition time are superior compared to the neutron scattering

EXAMPLE II

SAXS on single-Q and multi-Q textures in tetragonal Heusler alloy

In collaboration with TU Dresden and MPI CPfS

Tetragonal (D_{2d}) anti-skyrmion Heusler alloy $Mn_{1.4}PtSn$

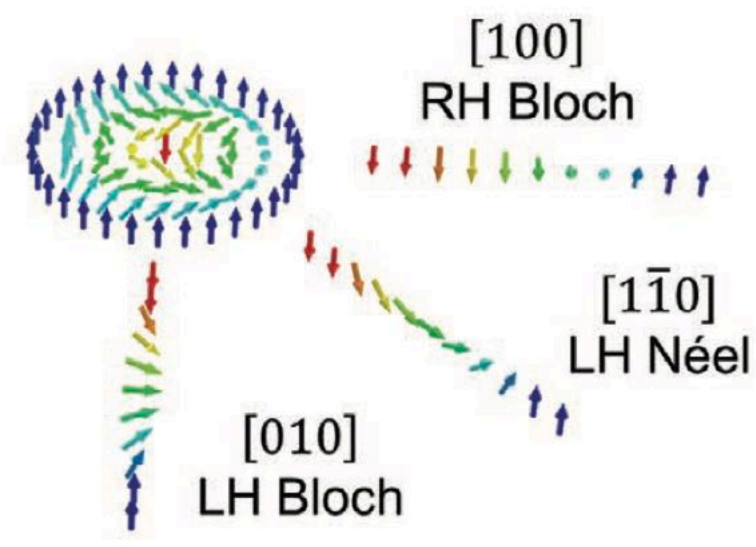

T. Ma, et al., Adv. Mater. **2020**, 32, 2002043

tilting of the spiral plane by the in-plane field

Ex-situ in-plane field training:

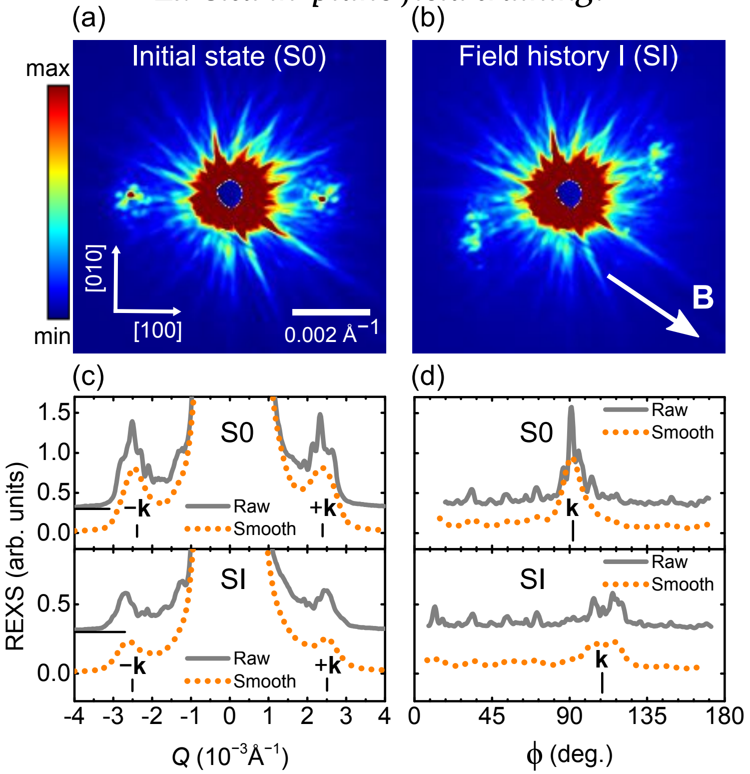

Actually depends on temperature

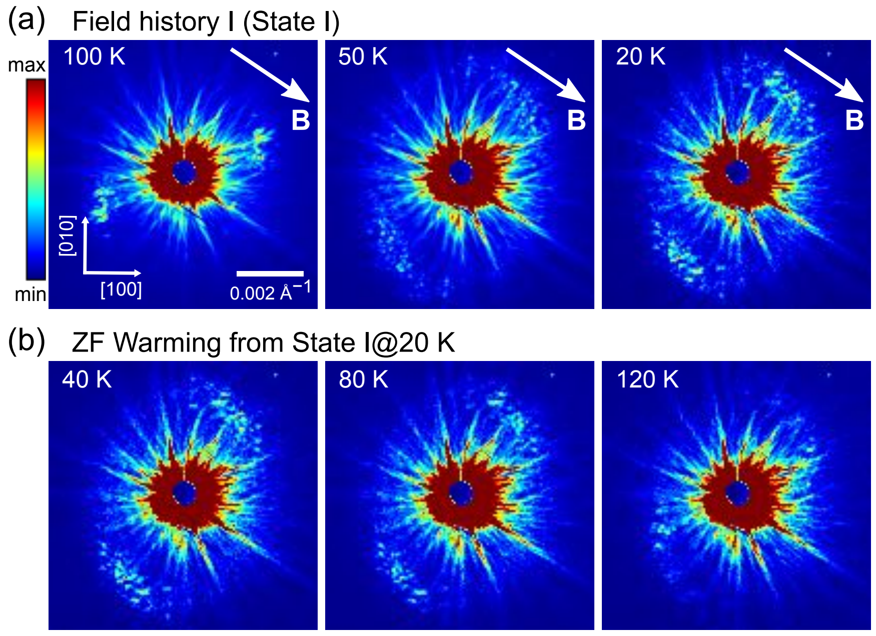

- Flexibility in the field orientation compared to Lorentz TEM: ex-situ in-plane field on D_{2d} $Mn_{1.4}PtSn$ at BOREAS (ALBA)
- The spiral moves towards orthogonal-to-the-field axis - typical to cycloid/stripe domain but it is unexpected for this symmetry group
- At low *T*s gets more 'cycloidal'

Dipolar interactions!

A. Sukhanov, V.U., et al. PRB 106, L140402 (2022)

EXAMPLE II

SAXS on single-Q and multi-Q textures in tetragonal Heusler alloy

In collaboration with TU Dresden and MPI CPfS

Tetragonal (D_{2d}) anti-skyrmion Heusler alloy $Mn_{1.4}PtSn$

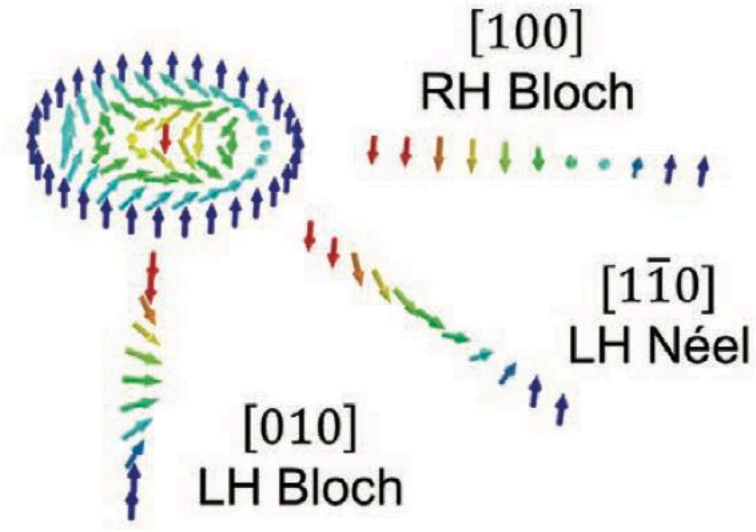

T. Ma, et al., Adv. Mater. **2020**, 32, 2002043

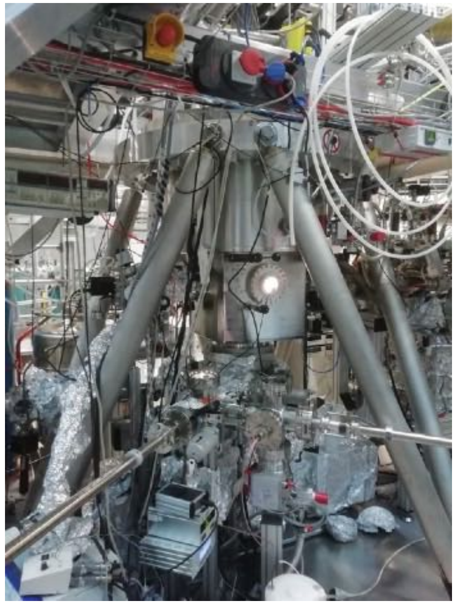

VEKMAG @ BESSY-II

Full rotation of the spiral plane by the in-plane field!

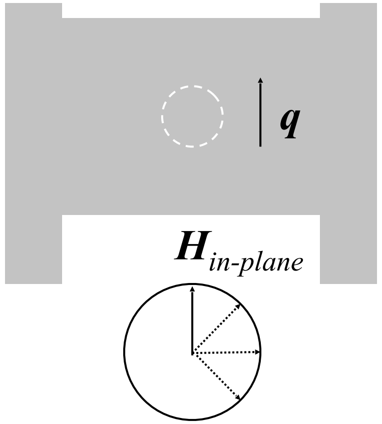

Summed over all azimuthal angles

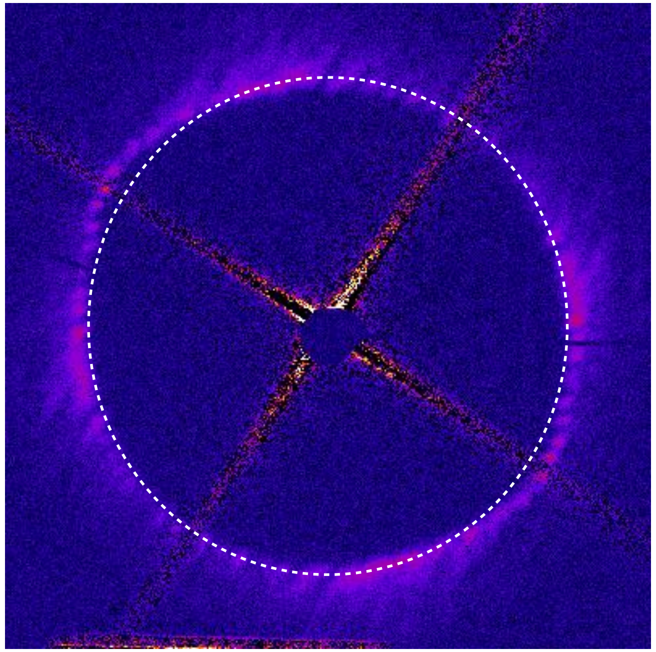

- Full control over the in-plane spiral propagation plane via vector magnetic field at VEKMAG (BESSY-II)
- At 300 K the spiral can be rotated freely within the tetragonal plane
- The *Q*-vector anisotropy depends on the sample shape

Dipolar interactions!

EXAMPLE II

SAXS on single-Q and multi-Q textures in tetragonal Heusler alloy

In collaboration with TU Dresden and MPI CPfS

History dependence of the spiral switching:

(1) Prepare a single domain by the corresponding in-plane field

(2) Apply a finite field in the direction of *k*

(3) The selected domain re-orients to the orthogonal direction

Orthogonal helices in a D_{2d} system have opposite chiralities (in principle)

↓

To change the helical propagation vector from [100] to [010] the system goes through an intermediate triple-Q state

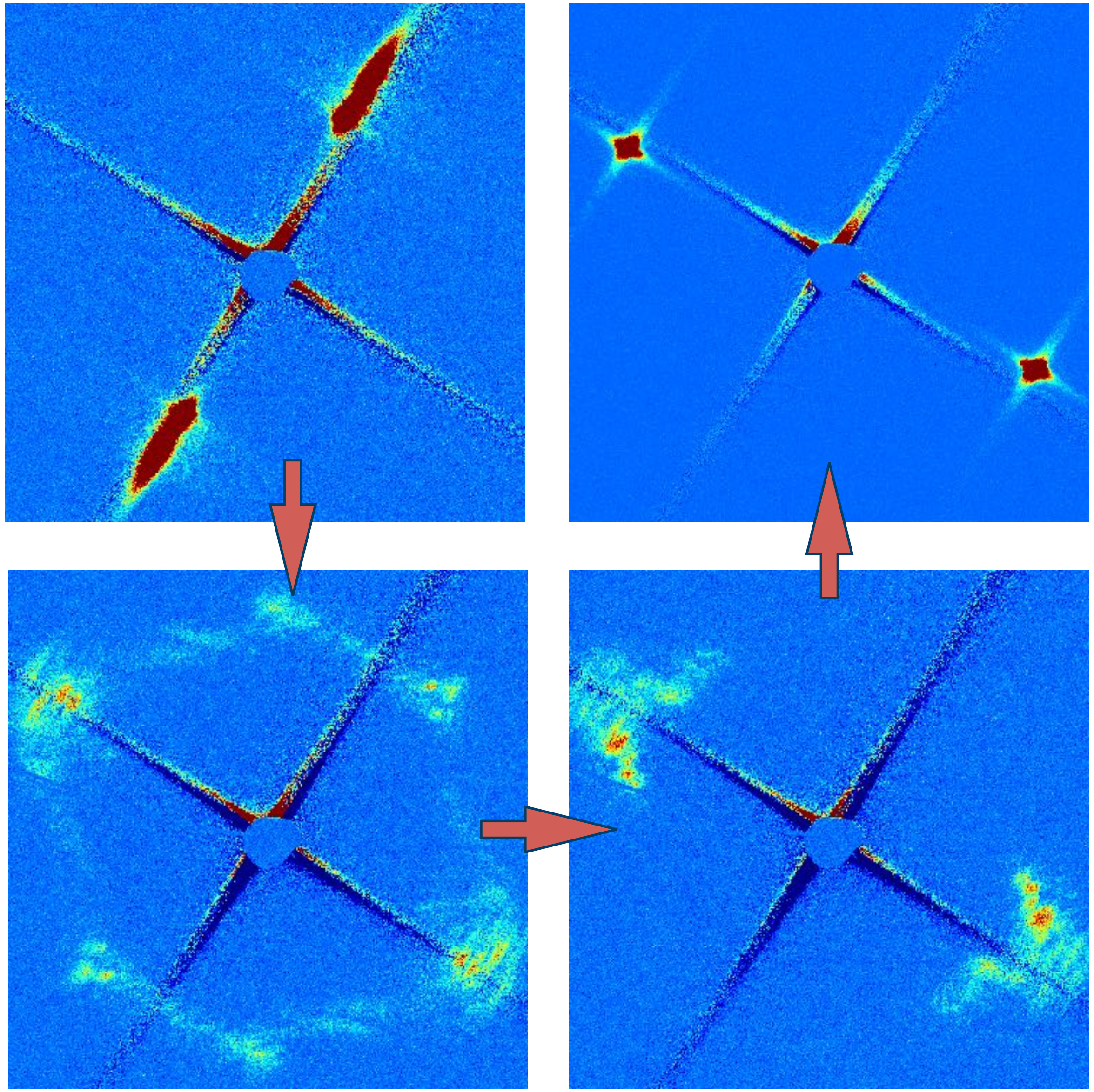

CONCLUSIONS

- ❑ Resonant SAXS is an excellent tool study long-periodic spin textures
- ❑ Element selectivity is naturally provided
- ❑ Flexible sample environment
- ❑ Sensitive to very small sample volumes, e.g. 1 x 1 x 0.1 μm^3
- ❑ Requires rather complex sample preparation
- ❑ Complementary to neutron scattering and electron microscopy

- ❑ Allows to extract weak parameters of the spin Hamiltonian (AEI) in cubic chiral magnets (FeGe, Cu_2OSeO_3, CoZnMn, FeCoSi, etc.)
- ❑ Adds new knowledge of the spin spiral behaviours in (not quite) D_{2d} systems

PHYSICAL REVIEW RESEARCH

Welcome Recent Subjects Accepted Collections Authors Referees Search About Scope Editorial Team

Accepted Paper

Direct observation of exchange anisotropy in the helimagnetic insulator Cu_2OSeO_3

Phys. Rev. Research

Priya R. Baral, Oleg I. Utesov, Chen Luo, Florin Radu, Arnaud Magrez, Jonathan S. White, and Victor Ukleev

PHYSICAL REVIEW B **106**, L140402 (2022)

Letter

Hybrid Bloch-Néel spiral states in $Mn_{1.4}PtSn$ probed by resonant soft x-ray scattering

A. S. Sukhanov,[1,*,†] V. Ukleev,[2,3,*,‡] P. Vir,[4] P. Gargiani,[5] M. Valvidares,[5] J. S. White,[2] C. Felser,[6] and D. S. Inosov[1,7]

Collaborators

ALBA synchrotron
P. Gargiani, M. Valvidares

École Polytechnique Fédérale de Lausanne
P.R. Baral, A. Magrez

Helmholtz-Zentrum Berlin
C. Luo, Y.-H. Wu, F. Radu

Technische Universität Dresden
A. Sukhanov, M. Winter, M. Rahn,
A. Tahn, D. Inosov, B. Rellinghaus

Paul Scherrer Institut
J.S. White

Institute for Basic Science
O.I. Utesov

Funding

Thank you for your attention!

SPICE
SPIN PHENOMENA
INTERDISCIPLINARY CENTER

victor.ukleev@helmholtz-berlin.de